Available online at www.sciencedirect.com

ScienceDirect

Physics of the Earth and Planetary Interiors 159 (2006) 118–126

PHYSICS OF THE EARTH AND PLANETARY INTERIORS

www.elsevier.com/locate/pepi

In situ X-ray diffraction study of the effect of water on the garnet–perovskite transformation in MORB and implications for the penetration of oceanic crust into the lower mantle

Asami Sano[a,*], Eiji Ohtani[a], Konstantin Litasov[a], Tomoaki Kubo[b], Tomofumi Hosoya[a], Kenichi Funakoshi[c], Takumi Kikegawa[d]

[a] *Institute of Mineralogy, Petrology and Economic Geology, Faculty of Science, Tohoku University, Sendai, Japan*
[b] *Department of Earth and Planetary Sciences, Faculty of Sciences, Kyushu University, Fukuoka, Japan*
[c] *Spring-8, Japan Synchrotron Radiation Research Institute, Kouto, Hyogo, Japan*
[d] *Photon Factory, High Energy Accelerator Research Organization, Tsukuba, Japan*

Received 26 August 2005; received in revised form 27 June 2006; accepted 17 July 2006

Abstract

The phase boundary of the transformation of garnet to perovskite in hydrous mid-ocean ridge basalt (MORB) was determined by in situ high-pressure and high-temperature X-ray diffraction (XRD) experiments. The garnet-bearing assemblage was formed in experiments at pressures below 21 GPa. In contrast, an assemblage of Mg-perovskite, Ca-perovskite, stishovite, CF phase and/or NAL phase is stable at pressures above 21 GPa. Garnet- and perovskite-bearing assemblages were synthesized at a pressure range of 20–25 GPa and a temperature range of 1000–1600 °C. On the basis of our results, we have located the garnet–perovskite phase boundary and find that it can be described by the following equation: P (GPa) = 0.004T (°C) + 17.5, which positions it 2 GPa lower under dry conditions. If the top 7 km of the slab is colder than 1200 °C in the transition zone, perovskite will appear at a depth shallower than that where ringwoodite decomposes. This result indicates that the MORB layer becomes denser than the peridotite portion of the slab throughout the transition zone and the lower mantle, and thus no density crossover would exist between basalt and underlying peridotite along the cold subducting slab geotherm.

Keywords: In situ X-ray diffraction; Mid-ocean ridge basalt (MORB); Density crossover; Slab; Garnet; Hydrous conditions

---

1. Introduction

It is believed that the subducting lithosphere consists of an upper mid-ocean ridge basaltic (MORB) layer and a lower peridotite layer (e.g., Poli and Schmidt, 2002). The mineral components in a subducting slab transform to high-pressure phases as the slab descends into the deep mantle. In the peridotite layer, the ringwoodite-bearing lithology transforms to a denser perovskite-bearing lithology at the base of the mantle transition zone. However, garnet, which is a major component of the MORB layer, survives to higher pressures (e.g., Irifune and Ringwood, 1993). This difference in the depth at which perovskite appears may cause a density crossover between the MORB layer and the surrounding mantle. As a result, the oceanic crust in the subducting slabs may become buoyant at the base of the transition zone to form a megalith (e.g., Ringwood, 1994).

---

[*] Corresponding author. Tel.: +81 22 795 6664; fax: +81 22 795 6675.
E-mail address: sano@ganko.tohoku.ac.jp (A. Sano).

0031-9201/$ – see front matter © 2006 Elsevier B.V. All rights reserved.
doi:10.1016/j.pepi.2006.07.004

While the garnet–perovskite transformation is important in the discussion of slab dynamics, there is disagreement about the location of the phase boundary. In dry MORB, Hirose and Fei (2002) used quench experiments to show that the transformation takes place at 26 GPa and concluded that there is no buoyancy deeper than 720 km. Irifune and Ringwood (1993), on the other hand, suggested that garnet can survive to a depth of 800 km. Recently, Litasov et al. (2004) conducted in situ X-ray diffraction studies and found that the phase boundary has a positive Clapeyron slope that is larger than that found in previous studies.

Subduction zone are regions where water is transported into the mantle by hydrous phases or defects in nominally anhydrous minerals (e.g., Ono, 1998). It is widely accepted that water has a great influence on the transport properties of minerals (e.g., Kubo et al., 2004) and phase relations (e.g., Litasov and Ohtani, 2005). Litasov and Ohtani (2005) used quench experiments to show that the liquidus phase in MORB changes in the presence of water, and that perovskite appears at pressures of about 1.5 GPa lower than that in a dry system. The purpose of this study is to determine the phase boundary of the garnet–perovskite transformation in hydrous MORB by in situ X-ray diffraction experiments and to discuss the effect of water on the fate of the subducting slab.

2. In situ X-ray diffraction experiments

In situ high-pressure and high-temperature X-ray diffraction experiments were performed using a 1500-ton uniaxial press (SPEED1500) at beamline BL04B1 at SPring-8 and a 700-ton uniaxial press (MAX III) at beamline BL14C at the Photon Factory. Sintered diamond anvils were used as the second-stage anvils for the experiments carried out at the Photon Factory, while tungsten carbide anvils were used in the experiments carried out at the SPring-8 facility. A white X-ray beam produced by synchrotron radiation was collimated through collimating slits; diffraction signals were collected by the energy dispersive method using a pure germanium solid-state detector with a fixed diffraction angle (2θ) of 5°. The diffraction angle was calibrated before and after the experiments using diffraction from a gold pressure marker.

The cell assembly used in the current study was similar to that of Litasov et al. (2004). The furnace assembly consisted of a cylindrical $LaCrO_3$ heater with a graphite X-ray transparent window in the central region. A Pd70%Ag30% alloy was chosen as the capsule material when the target temperature was lower than 1400 °C, whereas platinum was used at higher temperatures. Temperature was measured with a W3%Re–W25%Re thermocouple with no correction for the effect of pressure on the electromotive force (EMF) of the thermocouple. Pressure was calculated using equation of state of gold proposed by Anderson et al. (1989), Shim et al. (2002) and Tsuchiya (2003) using the observed unit cell volumes of gold. Gold powder was mixed with the sample in a 1:20 weight ratio of gold to sample when using the Pd70%Ag30% capsule. However, for the platinum capsule material, the gold powder was mixed with MgO and placed outside of the capsule. The pressure uncertainty is approximately 0.1–0.5 GPa. This figure was based on the uncertainty of the unit cell volume of gold, as calculated by the least squares approximation of the X-ray diffraction data.

Anhydrous glass with an average mid-ocean ridge basalt composition (Melson et al., 1976) was synthesized under a controlled oxygen fugacity of $\log f_{O_2} = 10^{-9}$. The chemical composition of the glass is shown in Table 1. The starting material was loaded in the capsule and distilled water (about 10% by weight) was added before welding the capsule.

For the Pd70%Ag30% alloy capsule, we determined the stable phases at each P–T condition using in situ X-ray diffraction method. The effect of transformation kinetics has been an important issue in determining phase relations using in situ X-ray diffraction. Furthermore, the transformation of garnet to perovskite is particularly sluggish (Kubo et al., 2002). To avoid the possibility of sluggish kinetics when crossing the garnet to perovskite phase boundary, we used synthesis experiments (except for run, S1314) in an effort to bracket the transition. Oil pressure was increased to a target sample pressure at ambient temperature, and the sample was then heated to a target temperature until the formation of either a garnet- or a perovskite-bearing assemblage was observed at a constant press load. We collected at least two sets of diffraction profiles, each with duration of 300–1000 s, at each pressure and at temperatures of 600–1500 °C. Diffraction patterns were constantly cross-checked with previous patterns to determine whether or not the formation of garnet or perovskite had occurred. In run S1314, we conducted an additional experiment, which crossed the phase boundary from the perovskite to garnet stability field, and found the results to be consistent with those of the synthesis runs.

When platinum was used as the capsule material for experiments at higher temperature, diffraction from the samples could not be detected because of the high X-ray absorption by the capsule. For these runs, we measured only the pressure at high-temperature using in situ X-ray

Table 1
Compositions of phases synthesized from the MORB starting material at 24.4 GPa and 1600 °C (Run S1102)

	S.M.	Mg-Pv	Ca-Pv	CF	NAL	St
SiO_2	51.0	33.4 (0.8)	47.7 (1.4)	25.5 (0.3)	18.4 (2.0)	96.0 (1.0)
TiO_2	1.5	3.3 (0.2)	2.6 (0.3)	1.0 (0.2)	0.9 (0.2)	0.1 (0.02)
Al_2O_3	15.7	15.8 (0.5)	4.0 (1.1)	37.9 (0.5)	45.9 (2.0)	3.0 (0.2)
FeO	9.8	26.5 (0.6)	2.6 (0.9)	13.5 (0.4)	10.8 (1.0)	0.3 (0.1)
MgO	7.7	17.8 (0.7)	2.0 (0.4)	9.8 (0.1)	15.2 (0.5)	0.1 (0.05)
CaO	11.5	1.4 (0.8)	38.3 (2.1)	1.4 (0.3)	2.3 (0.5)	0.2 (0.1)
Na_2O	2.7	0.4 (0.1)	0.7 (0.1)	9.8 (0.6)	5.3 (0.5)	n.d.
K_2O	0.2	n.d.	0.2 (0.2)	n.d.	0.6 (0.3)	n.d.
Total	100.0	98.6 (1.1)	98.0 (0.9)	98.9 (0.8)	99.4 (1.1)	99.6 (1.3)
O		3	3	12	12	2
Si		0.666	0.933	1.958	1.384	0.970
Ti		0.050	0.038	0.055	0.053	0.001
Al		0.373	0.093	3.430	4.088	0.036
Fe		0.443	0.042	0.866	0.681	0.003
Mg		0.529	0.057	1.121	1.709	0.001
Ca		0.029	0.802	0.116	0.182	0.002
Na		0.014	0.026	1.452	0.780	n.d.
K		n.d.	0.006	n.d.	0.059	n.d.
Cations		2.105	1.998	8.999	8.937	1.012

Abbreviations are as follows: S.M., starting material; Mg-Pv, Mg-perovskite; Ca-Pv, Ca-perovskite; CF, CF phase; NAL, NAL-phase; St, stishovite. Values in parentheses represent one standard deviation.

diffraction of the gold pressure standard. After heating for 60 min at high-pressure and high-temperature, samples were recovered and analyzed using a micro-beam X-ray powder diffractometer (MacScience M18XCE) and a micro-Raman spectrometer (Jasco NRS-2000). Chemical compositions of the recovered samples were analyzed with an electron microprobe (JEOL JXL8800M) with operating conditions of 15 kV and 10 nA.

3. Transformation of garnet to perovskite in hydrous MORB

Nine in situ X-ray diffraction experiments were carried out in the pressure range of 19.9–25.5 GPa at temperatures up to 1600 °C. In two experiments conducted at 1400 °C (S1334) and 1600 °C (S1102), we measured the pressure based on the in situ determination of the lattice parameter of gold, and the stable phase was identified by X-ray diffraction of the recovered samples. Fig. 1 and Table 2 summarize the experimental conditions and results. During the experiments, three phase assemblages were observed, namely, (1) Ca–Mg–Al (CMA)-perovskite and stishovite; (2) garnet, stishovite and an aluminous phase; and (3) Mg-perovskite, Ca-perovskite, stishovite and an aluminous phase. CMA-perovskite is an orthorhombic Ca–Mg–Al perovskite with a high Ca content, which is synthesized from a glass starting material (Funamori et al., 2000).

In all runs, with the exception of run mb51, we observed the appearance of a metastable CMA-perovskite phase with orthorhombic symmetry at 1000–1100 °C from the glass starting material during heating. The coexistence of stishovite with CMA-perovskite was observed only during one run (S1219). When the temperature was increased from 1100 to 1200 °C, CMA-perovskite decomposed into a garnet-bearing assemblage: garnet, stishovite and aluminous phases (calcium-ferrite type (CF) phase (Irifune and Ringwood, 1993) or $M_3Al_4Si_{1:5}O_{12}$ (M = Mg, Fe, Ca, Na, K) phase (NAL phase) (Miyajima et al., 1999)) in the runs at pressures below 21 GPa (mb41, S1221). We observed that garnet remained stable up to 22 GPa and 1300 °C. In contrast, CMA-perovskite decomposed into an assemblage of Mg-perovskite, Ca-perovskite, stishovite, CF phase and/or NAL phase in several other runs at pressures above 21 GPa. We could not distinguish between CF phase and NAL phase from the X-ray diffraction patterns, but electron microprobe analysis of the recovered samples suggests the existence of both phases (Table 1).

The presence of CMA-perovskite, which has a density between that of garnet and Mg-perovskite, is a matter of debate. Funamori et al. (2000) reported the formation of CMA-perovskite from glass starting material at 50 GPa, and concluded that this phase is stable in the subducting MORB layer at conditions prevalent in the lower mantle. Recently, it has been argued that this phase is

Table 2
Experimental conditions and results

T (°C)	P_{And} (GPa)	P_{Shim} (GPa)	P_{Tsu} (GPa)	Result
Run no. mb41				
1000	21.1 (0.2)	21.7	22.2	Glass → CMA
1100	20.9 (0.5)	21.6	22.0	CMA → Gt + St
1200	20.6 (0.1)	21.4	21.8	Gt + St
Run no. mb42				
1100	25.5 (0.3)	26.3	26.9	Glass → CMA
1200	24.8 (0.1)	25.6	26.1	CMA → MPv + CPv + Al + St
Run no. mb43				
1100	23.5 (0.3)	24.3	24.8	Glass → CMA
1200	23.1 (0.2)	23.9	24.4	CMA → MPv + CPv + Al + St
Run no. mb51				
1100	21.6 (0.2)	22.3	22.7	Glass → MPv + CPv + Al + St
Run no. S1219				
1100	24.1 (0.4)	24.8	25.4	Glass → CMA + St
1200	24.3 (0.5)	25.1	25.6	CMA → MPv + CPv + Al + St
1250	24.1 (0.5)	25.0	25.5	CMA → MPv + CPv + Al + St
1300	23.4 (0.5)	24.3	24.7	CMA → MPv + CPv + Al + St
1350	24.0 (0.4)	25.0	25.4	CMA → MPv + CPv + Al + St
1400	23.2 (0.1)	24.2	24.6	MPv + CPv + Al + St
1500	23.1 (0.3)	24.2	24.5	MPv + CPv + Al + St
Run no. S1221				
1000	20.3 (0.5)	20.9	21.3	Glass → CMA
1200	20.6 (0.3)	21.4	21.7	CMA → Gt + St + Al
1150	20.6 (0.3)	21.4	21.8	Gt + St + Al
1200	21.7 (0.3)	22.6	23.0	Gt + St + Al
1300	22.3 (0.5)	23.2	23.6	Gt + St + Al
Run no. S1314				
1000	23.0 (0.1)	23.6	24.1	Glass → CMA
1200	22.6 (0.1)	23.4	23.8	CMA → MPv + CPv + Al + St
1150	21.7 (0.2)	22.4	22.8	MPv + CPv + Al + St → Gt + CPv + St + Al
1200	21.8 (0.1)	22.7	23.1	MPv + CPv + Al + St → Gt + CPv + St + Al
Run no. S1102 (Pt capsule[a,b])				
1600	24.4 (0.1)	25.6	25.9	MPv + CPv + Al + St
Run no. S1334 (Pt capsule[a])				
1400	22.7 (0.5)	23.7	24.3	MPv + CPv + Al + St

CMA, CMA-perovskite; St, stishovite; Gt, garnet; MPv, Mg-perovskite; CPv, Ca-perovskite; Al, aluminous phase (calcium-ferrite type phase and/or NAL phase). Arrows indicate reaction from former mineral assemblage to latter mineral assemblage. All phases were coexisted with water rich fluid. Pressure was calculated based on the equation of state of gold by Anderson et al. (1989), P_{And}; Shim et al. (2002), P_{Shim}; Tsuchiya (2003), P_{Tsu}. The error of pressure in Anderson's scale is shown in parenthesis.

[a] In situ determination of pressure at high-temperature was made. Identification of the phases is made by EPMA, X-ray diffraction and Raman spectra of the recovered run products.

[b] Temperature was estimated by power–temperature relation.

metastable when glass was used as the starting material (Asahara et al., 2005). In the present study, we observed the disappearance of CMA-perovskite at 1200 °C. On the other hand, Asahara et al. (2005) found that it survives up to 1800 °C and 34 GPa, and Litasov et al. (2004) reported its survival up to 1300 °C and from 21 to 29 GPa under dry conditions. The temperature variations under which CMA-perovskite appears might be explained due to enhanced transformation kinetics by the presence of water. It is important to clarify whether CMA-perovskite is thermodynamically stable under low temperature conditions of the slabs, since it may play an important role in determining the density profile of the subducting slabs.

In one run (S1314), we carried out isothermal decompression until we observed the appearance of garnet following the growth of perovskite at 22.5 GPa

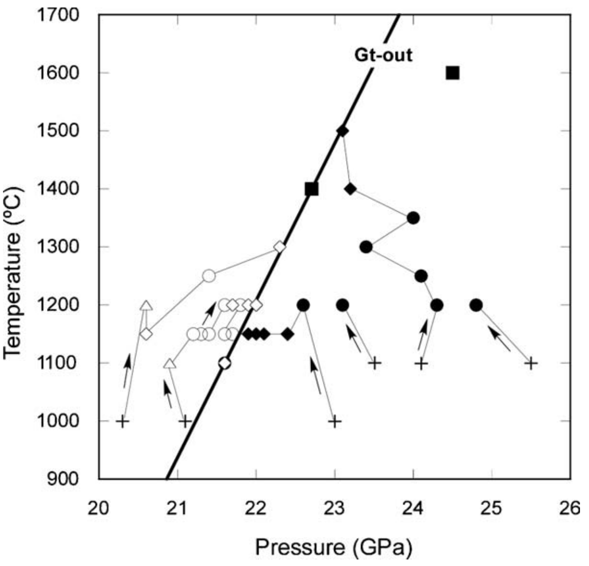

Fig. 1. Garnet–perovskite transformation in hydrous MORB. Dashed line represents the boundary of garnet disappearance in hydrous MORB, filled symbols indicate perovskite-bearing assemblage, open symbols indicate garnet-bearing assemblage, and crosses indicate existence of CMA-perovskite. Triangles represent transformation of CMA-perovskite to garnet, open circles represent transformation of perovskite to garnet and filled circles represent transformation of CMA-perovskite to Mg-perovskite bearing assemblage. Filled square symbols represent Mg-perovskite bearing assemblage from recovered sample which pressure was determined by in situ observation. Small diamonds represent conditions where no change in diffraction profiles occurred. Pressure was calculated from the equation of state of gold by Anderson et al. (1989).

and 1200 °C, for 10 min (Fig. 2b). Fig. 2 shows the change in diffraction patterns during decompression at high-temperatures. We observed the growth of garnet at 21.9 GPa and 1200 °C, after a duration of 23 min (Fig. 2c). After further decompression, Mg-perovskite finally disappeared at 21.1 GPa and 1000 °C (Fig. 2d). This apparent crossing of the phase boundary is consistent with the result of runs mb41–52 and S1314. We conclude that the transformation from perovskite to garnet is not kinetically inhibited, in contrast to the transformation of garnet to perovskite (Kubo et al., 2002).

We performed two synthesis experiments at temperatures higher than the melting temperature of the Pd70%Ag30% alloy capsule (S1102, S1334). The two recovered samples consisted of an assemblage containing Mg-perovskite (Fig. 3). The phase boundary is restricted to narrow pressure and temperature conditions at four data points as follows: where the garnet or perovskite assemblage was formed from CMA-perovskite or glass starting materials (S1221, mb51), perovskite transformed to garnet during isothermal decompression (S1314) and during the synthesis experiment at high-

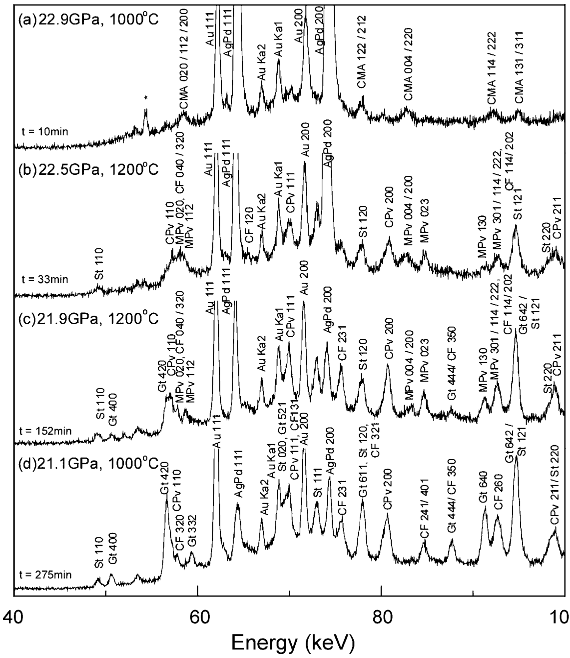

Fig. 2. Examples of X-ray diffraction profiles during a single run (Run S1314). (a) Appearance of CMA-perovskite after the increase in temperature from 1000 to 1200 °C. (b) Transformation of CMA-perovskite to Mg-perovskite bearing assemblage after decompression from 21.9 to 22.5 GPa at 1200 °C. (c) Appearance of garnet lithology after decompression from 22.5 to 21.9 GPa at 1200 °C. (d) Garnet-bearing lithology. CMA, CMA-perovskite; St, stishovite; CPv, Ca-perovskite; MPv, Mg-perovskite; CF, $CaFe_2O_4$-type aluminous phase; Gt, Garnet; *, unknown; *t*, time elapsed since reaching 22.9 GPa and 1000 °C where the condition of CMA-perovskite appears. The additional peaks are due to diffraction from the heater.

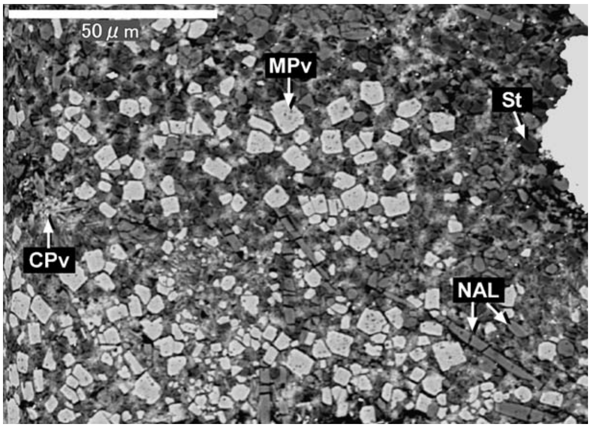

Fig. 3. Back-scattered electron image of recovered sample (S1102). St, stishovite; CPv, Ca-perovskite; MPv, Mg-perovskite; NAL, NAL phase.

Table 3
Lattice parameters and volumes of minerals of recovered samples

Phase	Lattice parameter (Å)	Volume (Å^3)
S1314 (recovered from 21.8 GPa, 1200 °C)		
Gt	$a = 11.58(3)$	1560.2(12)
St	$a = 4.179(3)$, $c = 2.680(3)$	46.80(8)
NAL	$a = 8.816(5)$, $c = 2.789(2)$	187.7(2)
CF	$a = 8.754(8)$, $b = 10.038(8)$, $c = 2.789(1)$	245.1(3)
S1219 (recovered from 23.1 GPa, 1500 °C)		
MPv	$a = 4.827(2)$, $b = 5.008(2)$, $c = 7.030(1)$	167.0(1)
St	$a = 4.179(5)$, $c = 2.700(5)$	46.63(1)
CF	$a = 8.742(4)$, $b = 10.111(3)$, $c = 2.781(1)$	245.8(2)

Abbreviations are the same as in Fig. 2.

temperatures (S1334). The uncertainty of the pressure for Anderson's pressure scale is given in Table 2. Thus, the phase boundary can be described by the following equation, P (GPa) = 0.004T (°C) + 17.5 based on the equation of state of gold by Anderson et al. (1989). Alternatively, it is described by P (GPa) = 0.005T (°C) + 17.2 using the equation of state of gold by Shim et al. (2002) and P (GPa) = 0.005T (°C) + 16.8 using that of Tsuchiya (2003). The uncertainty of the slope of the phase boundary based on Anderson's pressure scale is ±0.002 GPa/°C.

Table 3 presents refined unit cell parameters and the volumes of the minerals at ambient conditions for the samples recovered from 21.8 GPa and 1200 °C (S1314), and 23.1 GPa and 1500 °C (S1219). The zero pressure volume of Mg-perovskite is larger than that of pure $MgSiO_3$ perovskite, which is consistent with results of previous studies (Hirose and Fei, 2002; Litasov et al., 2004), due to high FeO and Al_2O_3 contents in Mg-perovskite. The intensity of diffraction lines from the NAL phase was stronger than from the CF phase when they coexisted with garnet. These diffraction lines were absent in the profile of the perovskite-bearing assemblage.

Chemical compositions of minerals recovered from 24.4 GPa and 1600 °C are presented in Table 1. The assemblage consists of Mg-perovskite, NAL phase, CF phase, stishovite and amorphous Ca-perovskite (Fig. 3). Mg-perovskite is remarkable for its higher Fe and lower Mg and Si contents when compared to the results from dry conditions (Litasov et al., 2004; Hirose and Fei, 2002), that is similar to the composition found in a previous study of hydrous MORB (Litasov and Ohtani, 2005).

4. Effect of water on subducted oceanic basalt

Fig. 4 shows a comparison of our results with those of previous studies. Although there is a discrepancy between the different pressure scales, the post-garnet phase boundary in hydrous MORB is 2 GPa lower than that of the dry phase boundary (Litasov et al., 2004), with a similar slope based on Anderson's pressure scale (Fig. 4A). It intersects the post-spinel phase boundary of Mg_2SiO_4 (Fei et al., 2004; Katsura et al., 2003) at about 22 GPa and 1200 °C, using the equation of state for gold by Anderson et al. (1989). Litasov and Ohtani (2005) reported that a garnet-bearing lithology transforms to a perovskite-bearing one at 25–26 GPa in MORB that contains 2 wt.% H_2O based on quench experiments; how-

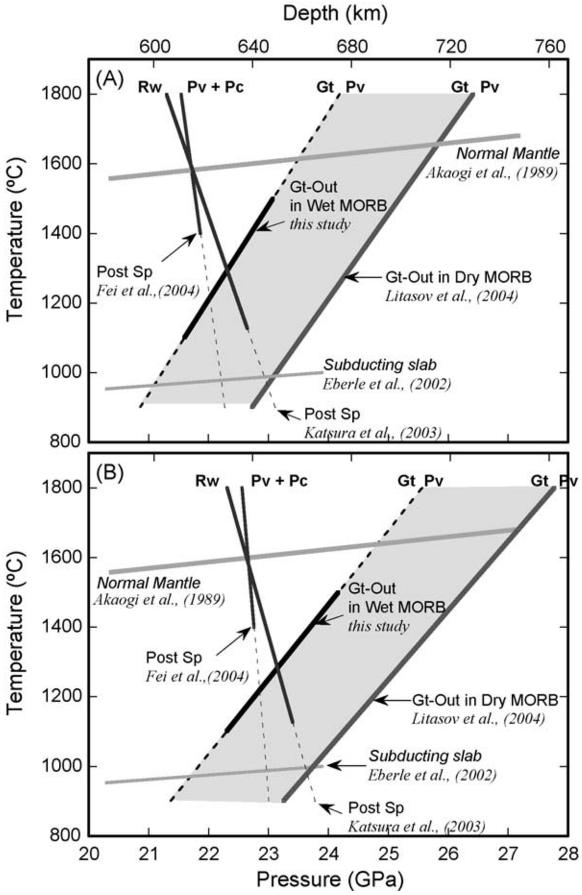

Fig. 4. Comparison of the garnet–perovskite phase boundary in the hydrous MORB determined in this study with that of dry MORB (Litasov et al., 2004) and the post-spinel phase boundary of Mg_2SiO_4 by Fei et al. (2004) and Katsura et al. (2003). The most negative slope was adopted of Katsura et al. (2003). (A) Pressures are based on the equation of state of Anderson et al. (1989). (B) Pressures are based on the equation of state of Shim et al. (2002). Post-spinel boundary is recalculated based on the equation of state of Shim et al. (2002). Dashed lines represent extrapolation. Normal mantle geotherm and temperature profile at surface of the subducting slab are from Akaogi et al. (1989) and Eberle et al. (2002), respectively. The shaded region represents the difference of the garnet–perovskite phase boundary between dry and hydrous MORB.

ever, we found this phase boundary at a pressure that is lower by 2 GPa. This inconsistency between the present study and that of Litasov and Ohtani (2005) may primarily be due to differences in the pressure scales. Litasov and Ohtani (2005) calibrated pressures in quench experiments based on the results of other quench experiments and in situ experiments, where the pressures were calculated by the equation of state of NaCl or platinum, or by the ruby fluorescence method. The equation of state of Anderson et al. (1989) is known to provide lower pressures than other pressure scales, such as that of platinum (e.g., Holmes et al., 1989).

Although there is uncertainty in the pressure scales, comparing the results made by the same experimental methods indicates that the shift of the phase boundary seems to be little affected by the total amount of water present. The shift of the phase boundary between dry MORB (Hirose and Fei, 2002) and MORB containing 2.0 wt.% H_2O system (Litasov and Ohtani, 2005) was 1.5 GPa in quench experiments, whereas it is 2.0 GPa in the in situ observations of this study and dry experiments (Litasov et al., 2004). These differences are similar within the uncertainties of the pressure scales. However, there remains the possibility that water escapes during experimentation. Water content in the recovered sample was difficult to quantify because the grain size is too small to analyze using IR spectroscopic methods.

The survival of garnet in the MORB layer is believed to cause a density crossover between the MORB layer and the lower peridotite layer of subducting slabs (Irifune and Ringwood, 1993). We are now able to present two possible scenarios for the behavior of hydrated slabs at a depth of around 660 km as a function of the slab geotherm: (1) if the geotherm of the top 7 km of the slab is located above the intersection of the post-spinel phase boundary of Mg_2SiO_4 in peridotite and garnet–perovskite phase boundary in wet MORB, there is a narrow depth interval of about 40 km for the density crossover. The oceanic crust becomes buoyant under these conditions; (2) if the geotherm of the MORB layer passes below the temperature of the intersection, the MORB layer becomes denser at a shallower depth than the post-spinel transformation and it can continue to penetrate into the lower mantle without accumulation as a garnetite megalith.

The disagreement over the different pressure scales for gold is also a matter of debate. The equation of state of Anderson et al. (1989) is known to provide lower pressure estimates than other pressure scales. Using the data from this study, the equation of state of gold of Shim et al. (2002) results in a phase boundary about 1 GPa higher (Fig. 4B) and that of Tsuchiya (2003) puts it about 1.5 GPa higher than of the boundary based on Anderson's scale. Thus, the intersection between the phase boundaries of the post-spinel and garnet–perovskite transitions in wet MORB is 22.8 GPa according to Shim's scale (Shim et al., 2002) (Fig. 4B) and 23.4 GPa according to Tsuchiya's scale (Tsuchiya, 2003), with both of them at about 1200 °C.

Shifts in phase boundaries due to the presence of water have been reported in several systems. For example, the phase boundary between olivine and wadsleyite in $(Mg, Fe)_2SiO_4$ shifts to a lower pressure in the presence of water (e. g., Chen et al., 2002; Litasov and Ohtani, 2003). This shift has been explained in terms of a difference in partitioning of water between these phases. However, the concentrations of water in majorite garnet and perovskite may be too low to explain such a large shift of the garnet–perovskite transition boundary, as suggested by the present study. Litasov and Ohtani (2005) provided an alternative explanation for the shift, suggesting that there is a change in the oxidation state due to the fluid. This is based on the observation that Mg-perovskite in hydrous MORB contains a higher Fe^{3+} content than in dry MORB (Litasov et al., 2003). Aluminous Mg-perovskite tends to contain more Fe^{3+} than garnet (McCammon, 1997) and thus the presence of fluid may oxidize the garnet-bearing lithology and enhance the formation of perovskite. This hypothesis is supported by chemical analyses in the present study (Table 1), which show that Mg-perovskite contains slightly higher FeO and Al_2O_3 than perovskite observed in the dry system (Litasov et al., 2005).

Another possible explanation is that the fluid can dissolve variable amounts of mantle components such as Mg and Si (e.g., Kawamoto et al., 2004), which may alter its mineral composition, resulting a change in the location of the phase transformation boundary. However, there is no information regarding the composition of the coexisting fluid at pressures above 20 GPa. Further studies are needed to clarify this problem.

Water is transported into the deep mantle by subducting slabs. In the upper mantle, lawsonite has been shown to be stable down to a depth of 300 km in a hydrated basaltic system. After the decomposition of lawsonite, there is no hydrous phase present in the MORB layer. However, aqueous fluid, released by the decomposition of hydrous phases, may be transported into the deep mantle as a trapped fluid without percolation due to the large dihedral angle between garnet and fluid (Ono et al., 2002). In addition, majoritic garnet and Al-bearing stishovite, which are the major components of MORB in the upper mantle and transition zone, can contain 1250 ppm OH and 840 ppm H_2O (Katayma et al., 2003;

Chung and Kagi, 2002), respectively. In the underlying peridotite layer, which comprises a large part of the slab, phase E, superhydrous phase B and phase D are stable as the slab descends into the transition zone. These dense hydrous magnesium silicate phases bring with them the capacity for a great deal of water content in the peridotite layer of 2 wt.% in a hot slab and 10 wt.% in a cold slab at the transition zone (Ohtani et al., 2004). Seismic observation implies that some slabs stagnate at the transition zone (e.g., Fukao et al., 2001) The stagnation of the slab should cause a rise in the slab temperature and dehydrate the peridotite layer. This, in turn, would cause shift the transformation of garnet to perovskite in the MORB layer to occur at a shallower depth, and the oceanic crust would penetrate into the lower mantle without separation from the peridotite layer near the depth of 660 km.

Acknowledgements

We thank A. Suzuki, H. Terasaki, T. Kawazoe, K. Tsuno, R. Ando and S. Kato for technical support during in situ X-ray diffraction experiments and T. Kondo for valuable advice. We appreciate two anonymous reviewers for their constructive reviews that improved the manuscript. This study was conducted at SPring-8 (Proposal no. 2002A0298-ND2-np, 2002B0566-CD2-np, 2004B0644-ND-2b) and Photon Factory (Proposal no. 2001G060). This work was financially supported by the Grant-in-Aid of the Scientific Research on Priority Areas (B) (no. 16075202) and Scientific Research (S) (no. 14102009) of the Ministry of Education, Culture, Sports, Science and Technology of the Japanese Government to E.O., and conducted as part of the 21st Century Center-of-Excellence program “Advanced Science and Technology Center for the Dynamic Earth”.

References

Akaogi, M., Ito, E., Navortsky, A., 1989. Olivine-modified spinel-spinel transitions in the system Mg_2SiO_4–Fe_2SiO_4: calorimetric measurements, thermochemical calculation, and geophysical application. J. Geophys. Res. 94 (B11), 15,671–15,685.

Anderson, O.L., Donald, G.I., Yamamoto, S., 1989. Anharmonicity and the equation of state for gold. J. Appl. Phys. 65 (4), 1534–1543.

Asahara, Y., Ohtani, E., Kondo, T., Kubo, T., Miyajima, N., Nagase, T., Fujino, K., Yagi, T., Kikegawa, T., 2005. Formation of metastable cubic-perovskite in high-pressure phase transformation of Ca(Mg, Fe, Al)Si_2O_6. Am. Mineral. 90, 457–462.

Chen, J., Inoue, T., Yurimoto, H., Weidner, D.J., 1875. Effect of water on olivine-wadsleyite phase boundary in the $(Mg, Fe)_2SiO_4$ system. Geophys. Res. Lett. 29 (18), doi:10.1029/2001GL014429.

Chung, J.I., Kagi, H., 2002. High concentration of water in stishovite in the MORB system. Geophys. Res. Lett. 29 (21), 2020, doi:10.1029/2002GL015579.

Eberle, M.A., Grasset, O., Sotin, C., 2002. A numerical study of the interaction between the mantle wedge, subducting slab, and overriding plate. Phys. Earth Planet. Int. 134, 191–202.

Fei, Y., Van Orman, J., Li, J., van Westrenen, W., Sanloup, C., Minarik, W., Hirose, K., Komabayashi, T., Walter, M., Funakoshi, K., 2004. Experimentally determined postspinel transformation boundary in Mg_2SiO_4 using MgO as an internal pressure standard and its geophysical implications. J. Geophys. Res. 109, B02305, doi:10.1029/2003JB002562.

Fukao, Y., Widiyantoro, S., Obayashi, M., 2001. Stagnant slabs in the upper and lower mantle transition region. Rev. Geophys. 39, 291–323.

Funamori, N., Jeanloz, R., Miyajima, N., Fujino, K., 2000. Mineral assemblages of basalt in the lower mantle. J. Geophys. Res. 105 (B11), 26037–26043.

Hirose, K., Fei, Y., 2002. Subsolidus and melting phase relations of basaltic composition in the uppermost lower mantle. Geochim. Cosmochim. Acta 66, 2099–2108.

Holmes, N.C., Moriarty, J.A., Gathers, G.R., Nellis, W.J., 1989. The equation of state of platinum to 660 GPa (6.6 Mbar). J. Appl. Phys. 66, 2962–2967.

Irifune, T., Ringwood, A.E., 1993. Phase transformations in subducted oceanic crust and buoyancy relationships at depth of 600–800 km in the mantle. Earth Planet. Sci. Lett. 117, 101–110.

Katayma, I., Hirose, K., Yurimoto, H., Nakashima, S., 2003. Water solubility in majoritic garnet in subducting oceanic crust. Geophys. Res. Lett. 30 (22), 2155, doi:10.1029/2003GL018127.

Katsura, T., Yamada, H., Shinmei, T., Kubo, A., Ono, S., Kanzaki, M., Yoneda, A., Walter, M.J., Ito, E., Urakawa, S., Funakoshi, K., Utsumi, W., 2003. Post-spinel transformation in Mg_2SiO_4 determined by high *P–T* in situ X-ray diffractometry. Phys. Earth Planet. Int. 136, 11–24.

Kawamoto, T., Matsukage, K.N., Mibe, K., Isshiki, M., Nishimura, K., Ishimatsu, N., Ono, S., 2004. Mg/Si ratios of aqueous fluids coexisting with forsterite and enstatite based on the phase relations in the Mg_2SiO_4–SiO_2–H_2O system. Am. Mineral. 89, 1433–1437.

Kubo, T., Shimojuku, A., Ohtani, E., 2004. Mg–Fe interdiffusion rates in wadsleyite and the diffusivity jump at the 410-km discontinuity. Phys. Chem. Miner. 31, 456–464.

Kubo, T., Ohtani, E., Kondo, T., Kato, T., Toma, M., Hosoya, T., Sano, A., Kikegawa, T., Nagase, T., 2002. Metastable garnet in oceanic crust at the top of the lower mantle. Nature 420, 803–806.

Litasov, K., Ohtani, E., 2005. Phase relations in hydrous MORB at 18–28 GPa: implications for heterogeneity of the lower mantle. Phys. Earth Planet. Int. 150, 239–263.

Litasov, K., Ohtani, E., Suzuki, A., Kawazoe, T., Funakoshi, K., 2004. Absence of density crossover between basalt and peridotite in the cold slabs passing through 660 km discontinuity. Geophys. Res. Lett. 31, L24607, doi:10.1029/2004GL021306.

Litasov, K., Ohtani, E., Langenhorst, F., Yurimoto, H., Kubo, T., Kondo, T., 2003. Water solubility in Mg-perovskites and water storage capacity in the lower mantle. Earth Planet. Sci. Lett. 211, 189–203.

Litasov, K., Ohtani, E., 2003. Stability of various hydrous phases in CMAS pyrolite-H_2O system up to 25 GPa. Phys. Chem. Miner. 30, 147–156.

McCammon, C., 1997. Perovskite as a possible sink for ferric iron in the lower mantle. Nature 387, 694–696.

Melson, W.G., Vallier, T.L., Wright, T.L., Byerly, G., Nelen, J., 1976. Chemical diversity of abyssal volcanic glass erupted along Pacific, Atlantic, and Indian ocean sea-floor spreading centers. In: Sutton, G.H., Manghnani, M.H., Moberly, R. (Eds.). The Geophysics of the Pacific Ocean Basin and Its Margin. Am. Geophys. Union, Geophys Monogr. Ser., vol. 19, pp. 351–367.

Miyajima, N., Fujino, K., Funamori, N., Kondo, T., Yagi, T., 1999. Garnet–perovskite transformation under conditions of the Earth's lower mantle: an analytical transmission electron microscopy study. Phys. Earth Planet. Int. 116, 117–131.

Ohtani, E., Litasov, K., Hosoya, T., Kubo, T., Kondo, T., 2004. Water transport into the deep mantle and formation of a hydrous transition zone. Phys. Earth Planet. Int. 143, 255–269.

Ono, S., 1998. Stability limits of hydrous minerals in sediment and mid-ocean ridge basalt compositions: Implications for water transport in subduction zones. J. Geophys. Res. 103 (B8), 18253–18268.

Ono, S., Mibe, K., Yoshino, T., 2002. Aqueous fluid connectivity in pyrope aggregates: water transport into the deep mantle by a subducted oceanic crust without any hydrous minerals. Earth Planet. Sci. Lett. 203, 895–903.

Poli, S., Schmidt, M.W., 2002. Petrology of subducted slabs. Annu. Rev. Earth Planet. Sci. 30, 207–235.

Ringwood, A.E., 1994. Role of the transition zone and 660 km discontinuity in mantle dynamics. Phys. Earth Planet. Int. 86, 5–24.

Shim, S., Duffy, T.S., Takemura, K., 2002. Equation of state of gold and its application to the phase boundaries near 660 km depth in Earth's mantle. Earth Planet. Sci. Lett. 203, 729–739.

Tsuchiya, T., 2003. First-principles prediction of the P–V–T equation of state of gold and the 660-km discontinuity in Earth's mantle. J. Geophys. Res. 108 (B10), 2462, doi:10.1029/2003JB002446.